

Inverse Method Using Finite Strain Measurements to Determine Flight Load Distribution Functions

Cameron W. Coates* and Priya Thamburaj†

Armstrong Atlantic State University, Savannah, Georgia 31419

DOI: 10.2514/1.21905

This work seeks to identify in-flight loads based on real-time data provided by strain gauges. Flight loads are identified based on an inverse interpolation method that uses results from a finite element model developed in I-DEAS software. The inverse interpolation is based on minimization of the error between calculated versus measured strains. Finite element strains are used as representative of measured strains for input into the analysis. Strains determined from surface loads of individual Fourier terms are also determined from the finite element model. Strain data from the applied unknown load coupled with finite element model data from the Fourier loads allow prediction of the Fourier coefficients of the actual load. Predicted Fourier coefficients are compared to sets of Fourier coefficients from a database based on historical or theoretical loads and a “least-squares” minimization performed to determine which set of coefficients are most probable. Successful load predictions are made for polynomial surface functions of one and two independent variables, using single and double Fourier series, respectively. It is shown that the variance of the strain data from individual loads plays a key role in the accuracy of the method.

I. Introduction

STRUCTURAL health monitoring is becoming increasingly important in military and civilian aerospace applications. Civilian airlines seek to extend the service, safety, and capability of an aging aircraft fleet while military aircraft are subjected to more diverse missions. Combat operations involve an increasing use of autonomous unmanned aircraft. The identification of real-time flight loads may be advantageous in several ways; for example, the information can be used to improve fatigue or critical load damage modeling or to improve aircraft handling or pilot response to unusual loads. Autonomous vehicles may use this information to make flight adjustments or to detect and quantify damage while in flight. This type of flight load information will also provide reliable databases, which may be used in a condition based maintenance program. The measurement of real-time flight loads, displacements, and stresses is typically very difficult due to the complexity of load measurement instrumentation.

This work proposes the application of an inverse method to develop a database of Fourier coefficients that will enable effective modeling of real-time flight loads. Because loads, stresses, and displacements are determined using experimentally measured structural response, the problem may result in a set of ill-posed governing equations. Hence a finite element based inverse method is chosen to predict the “best” solution. In this method, data obtained from a finite element analysis (FEA) will be used as measured data and analyzed to predict real-time flight loads. The strains could be measured with a fiber-optic sensor network, microelectromechanical system (MEMS) strain gauges, or typical strain gauges.

Several authors have developed various inverse methods to predict loads or displacements based on strain data. Shkarayev et al. [1] developed a finite element based methodology involving an inverse formulation that employs measured surface strains to recover the applied loads, stresses, and displacements in real time. The parameters of load interpolation were computed using a least-squares minimization procedure. These authors suggested that a quality

function be implemented to determine the actual load case. This quality function would be based on experimental statistics. Some numerical test cases were successfully performed, however, no supporting experiments were performed. Coates and Thamburaj [2] investigated this method’s efficacy if the load distribution functions of one and two variables were expressed as the sum of their single Fourier cosine series terms. Measured strain data were simulated with a finite element model, which was used as input to the inverse methodology. It was shown that if a database containing the Fourier coefficients of historical functions exists, the most probable load distribution function could be identified in real time using finite strain measurements. However, as the number of terms was increased or the functions of two variables increased in complexity the methodology lost accuracy.

Maniatty et al. [3] investigated solutions for inverse elastic and elastoviscoplastic problems based on the finite element method. Their method used a regularization procedure to impose smoothness on the solution. Maniatty and Zabarar [4] also more recently applied the regularization procedure coupled with a statistical approach initially developed by Tarantola [5]. The iterative nature of this method increases vulnerability to convergence problems and high computation costs. Bogert et al. [6] implemented an algorithm for recovering the displacement of a structure under arbitrary static loading using strain data determined at discrete locations. The solution was based on a modal transformation that uses the structure’s deformation and strain modes. Deformed shapes reconstructed from the modal transformation algorithm showed good agreement with the directly measured quantities. Kirby et al. [7] successfully demonstrated shape recovery for a beam based on strain data using an inverse method. The method employed directly integrated the strain displacement relationships using a polynomial representation of the strain field. Tessler and Spangler [8] implemented a smoothing functional which employs least-squares difference terms for interpolated element level strains and measured strains. The minimization of this functional forms the basis for an inverse finite element method being developed. Cao et al. [9] used a learning algorithm for a multilayer neural network to determine load strain relationships. Selection of the combination of learning parameters significantly affects convergence of the network. Convergence was therefore vulnerable to improper selection of combinations of these parameters.

This paper seeks to extend the work in [2] by approximating load distribution functions of two variables with their double Fourier series representation and to recover the Fourier coefficients of historical loads from finite strain measurements. This work also

Received 19 December 2005; revision received 14 March 2007; accepted for publication 15 March 2007. Copyright © 2007 by the American Institute of Aeronautics and Astronautics, Inc. All rights reserved. Copies of this paper may be made for personal or internal use, on condition that the copier pay the \$10.00 per-copy fee to the Copyright Clearance Center, Inc., 222 Rosewood Drive, Danvers, MA 01923; include the code 0021-8669/08 \$10.00 in correspondence with the CCC.

*Assistant Professor, Engineering Studies Department, Member AIAA.

†Assistant Professor, Engineering Studies Department.

explores the statistical aspects of the multiple least-squares regression model employed. The necessary confidence intervals, their relationship to the variance, and number of data points are also examined in order to characterize the robustness of the method.

II. Inverse Interpolation Method

A brief review of Shkarayev's method is provided; for more details the reader is encouraged to consult [1]. Consider an aircraft wing subjected to internal and external load changes. If strain gauges are placed on the wing at n specified locations, the strain data may be stored and used as input to an inverse analysis to determine the real-time load changes. A finite element model of the wing structure would have to be available because the method depends on finite element results.

From a set of m possible load cases, the i th load approximation may be expressed in parametric form

$$F_i(s) = \sum_{j=1}^l a_{ij} R_{ij}(s) \quad (1)$$

where the a_{ij} s are unknown approximation parameters and the $R_{ij}(s)$ are spatial distribution functions. By using Eq. (1) in the finite element method, the displacements $\{U\}$, strains $\{\varepsilon\}$, or stresses $\{\sigma\}$ corresponding to the i th load may be computed from

$$\{A_i\} = \sum_{j=1}^l a_{ij} \{A_{ij}\} \quad (2)$$

where A represents any of these parameters. If ε_i^* represents the measured strains for the i th load case, and ε_i represents the strains derived from applying each R_{ij} load case, the coefficients in Eq. (1) may then be computed by performing a least-squares minimization with respect to the parameter a_{ij} , where

$$S_i = \{\varepsilon_i - \varepsilon_i^*\}^T \{\varepsilon_i - \varepsilon_i^*\} = \left\{ \sum_{j=1}^m a_{ij} \{\varepsilon_{ij}\} - \varepsilon_i^* \right\}^T \left\{ \sum_{j=1}^m a_{ij} \{\varepsilon_{ij}\} - \varepsilon_i^* \right\} \quad (3)$$

This minimization can also be performed while accounting for certain inequity constraints. In this work, the R_{ij} terms are either single or double Fourier terms and will therefore always be known (excluding their coefficients). The current model considers the aircraft wing (semispan) under a cantilever condition. The surface load $p(x, y)$ may then be expressed (double Fourier) as

$$p(x, y) \cong a_{00} + \sum_{m=1}^{\infty} a_{0m} \cos\left(\frac{m\pi y}{K}\right) + \sum_{n=1}^{\infty} a_{n0} \cos\left(\frac{n\pi x}{L}\right) + \sum_{n=1}^{\infty} \sum_{m=1}^{\infty} a_{nm} \cos\left(\frac{n\pi x}{L}\right) \cos\left(\frac{m\pi y}{K}\right) \quad (4)$$

The database will consist of the a_{ij} Fourier coefficients from m possible load cases determined from historical or theoretical data. The a_{ij} s are stored in a matrix $[A]$ where

$$[A] = [\{a\}_1^* \{a\}_2^* \{a\}_3^* \cdots \{a\}_m^*] \quad (5)$$

Based on the load history, we can also represent the weighting constraints by w_i such that a weight matrix $[w]$ is expressed as

$$[w] = [w_1 \ w_2 \ w_3 \ \cdots \ w_m] \quad (6)$$

If an unknown load produces a set of strain values, these values may be used in Eq. (3) to obtain the Fourier coefficients $\{a\}$ of the unknown load. Using a least-squares minimization of the errors between the derived Fourier coefficients and the database sets of coefficients, we obtain

$$S_i = [\{a\}_i^* - \{a\}]^T [\{a\}_i^* - \{a\}] \quad (7)$$

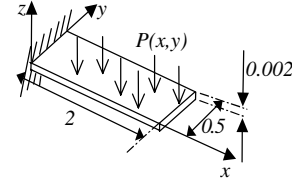


Fig. 1 Geometry, loading, and coordinate system of the finite element model.

$$S_w = (1 - w_i) S_i \quad (8)$$

The minimization of Eq. (7) coupled with weighted criteria from Eq. (8) provides the a_{ij} for the Fourier cosine series most representative of the loading. Several cases were analyzed and are discussed in Sec. IV. A robust linear regression algorithm employing the bisquare function was used in this work. If ε_i^* represents the measured strains for the i th load case, the residual or error between the predicted and measured strains can be written as

$$r_i = \{\varepsilon_i - \varepsilon_i^*\} = \left\{ \sum_{j=1}^m a_{ij} \{\varepsilon_{ij}\} - \varepsilon_i^* \right\} \quad (9)$$

The coefficients a_{ij} may then be computed by performing a least-squares minimization of the following:

$$S_r = w_i (r_i^T r_i) \quad (10)$$

where w_i represents a weighting function. In the robust linear regression, the least-squares solution was iteratively reweighted by applying the bisquare function shown in Eq. (11) to the residuals of the previous iteration:

$$w_i = [\text{abs}(r_i) < 1] (1 - r_i^2)^2 \quad (11)$$

III. Finite Element Model

The finite element model was developed using the I-DEAS commercial software. The model was discretized with a 64×16 mesh using the thin shell linear quadrilateral element of thickness 0.002. The bending stiffness for this element is based on the Mindlin shell equations in which the displacement due to transverse shear strain is included. The material property values used were Young's modulus $E = 72$ GPa and Poisson's ratio, $\nu = 0.3$. Seventeen uniformly spaced locations were selected along the line $y = 0.375$ and 17 selected along the line $x = 1.25$ to measure strain values ε_x and ε_y ; these strains correspond to the ε_i^* in Eq. (5). The surface loads are applied at the top of the shell element ($z = 0$). The cantilever dimensions were $2 \times 0.5 \times 0.002$ m³. The geometry, loading direction, and coordinate system are illustrated in Fig. 1.

IV. Numerical Simulations

A. Known Function Recovery

Several functions were recovered in [2] based on their R_{ij} terms. Some of these functions are provided in Table 1 as a reference. An inspection of Table 1 indicates that the estimates of the coefficients of y and y^2 were the least accurate for the polynomials

$$p_6(x, y) = L - Lx + \frac{x^2}{L} + K - Ky + \frac{y^2}{K}$$

and

$$p_4(x, y) = K - Ky + \frac{y^2}{K}$$

where $L = 2$ and $K = 0.5$. The y and y^2 coefficient terms for the function $p_6(x, y)$ were therefore investigated to discover the reasons for the inaccuracy. For the above-mentioned cases, the most likely sources of error for the y and y^2 coefficients were either that the number of strain values sampled from the y and y^2 distributions was

Table 1 Polynomial coefficients recovered using the inverse method for various functions

Type of load ($L = 2, K = 0.5$)	1	x	x^2	y	y^2
$p_1(x, y) = L - \frac{x}{L}$	1.9985	-0.4989	—	—	—
$p_2(x, y) = K - \frac{y}{K}$	0.5032	—	—	-2.0129	—
$p_3(x, y) = L - Lx + \frac{x^2}{L}$	1.9981	-1.9981	0.4996	—	—
$p_4(x, y) = K - Ky + \frac{y^2}{K}$	0.4936	—	—	-0.4233	1.8462
$p_5(x, y) = L - \frac{x}{L} + K - \frac{y}{K}$	2.5020	-0.4990	—	-2.0138	—
$p_6(x, y) = L - Lx + \frac{x^2}{L} + K - Ky + \frac{y^2}{K}$	2.4749	-1.9955	0.4987	-0.2599	1.5373

Table 2 Functions used to create a database and their Fourier coefficients

$p(x, y)$	$10(2-x)y(0.5-y)$	$2.5-0.5x-2y$	$10(2-x)y$	$10e^{-x-y}$	$2+3xy^2$
a_{00}	0.4167	1.5	2.5	3.4022	2.25
a_{n01}	0.3377	0.4053	2.0264	2.5767	-0.2026
a_{n02}	0	0	0	0.626	0
a_{n03}	0.0375	0.045	0.2252	0.385	-0.0225
a_{0m1}	0	0.4053	-2.0264	0.6863	-0.304
a_{0m2}	-0.2533	0	0	0.0428	0.076
a_{0m3}	0	0.045	-0.2252	0.078	-0.0338
a_{nm11}	0	0	-1.6426	0.5198	0.2464
a_{nm12}	-0.2053	0	0	0.0324	-0.0616
a_{nm13}	0	0	-0.1825	0.0591	0.0274
a_{nm21}	0	0	0	0.1263	0
a_{nm22}	0	0	0	0.0079	0
a_{nm23}	0	0	0	0.0143	0
a_{nm31}	0	0	-0.1825	0.0777	0.0274
a_{nm32}	-0.0228	0	0	0.0048	-0.0068
a_{nm33}	0	0	-0.0203	0.0088	0.003

insufficient or the variance of these strain data was not large enough or both.

These postulates were examined using the data set employed by the least-squares method to obtain the constant (for $R_{ij} = 1$) and the y coefficient within the function $p_6(x, y)$ (Table 1). The 95% confidence interval for estimating $p+1$ coefficients from n data points is found from

$$\hat{\beta}_i \pm t_{n-p-1, 0.025} \cdot s_{\hat{\beta}_i} \quad (12)$$

where $\hat{\beta}_i$ are the multiple least-squares estimates, $t_{n-p-1, 0.025}$ represents the student's t distribution with $n-p-1$ degrees of freedom, and $s_{\hat{\beta}_i}$ is the standard deviation of the $\hat{\beta}_i$ [10,11]. The number of strain data points used to generate the polynomial load distribution coefficients (R_{ij} s) was incrementally increased from 6 to 34 and the 95% confidence interval was observed to decrease accordingly. Figures 2 and 3 illustrate the decreasing 95% confidence interval for the constant (2.5) and the coefficient of y for $p_6(x, y)$. The calculated $\hat{\beta}_i$ approaches the actual β_i for both terms as expected; however, at 34 data points the y -coefficient $\hat{\beta}_i$ misses its

target value by 23% while the constant $\hat{\beta}_i$ is off its target value by 1%. The variance of the strain data set required to calculate the y coefficient is several orders of magnitude smaller than the variance of the strain data set required for the constant (coefficient of 1). This results in a larger 95% confidence interval as well as a poor estimate of β_i using 34 data points. Several more test runs at random locations indicated that a smaller data set with a variance on the same order of magnitude of larger data sets yields comparable confidence intervals. Therefore, to recover coefficients most accurately, the number of data points used should be maximized or data point locations should be chosen such that the variance value is comparable to the variance of previously successful data sets. The latter approach will be more cost effective and is therefore recommended.

B. Function Recovery from Database

Strains from specific functions acting as load distributions were entered in Eq. (3) as the $\{\varepsilon_i^*\}$. The functions chosen to illustrate double Fourier approximations were $10(2-x)y(0.5-y)$, $2.5-0.5x-2y$, $10(2-x)y$, $10e^{-x-y}$, and $2+3xy^2$. The Fourier coefficients obtained, shown in Table 2, were used to create pseudodatabases to investigate the efficacy of the method. In a

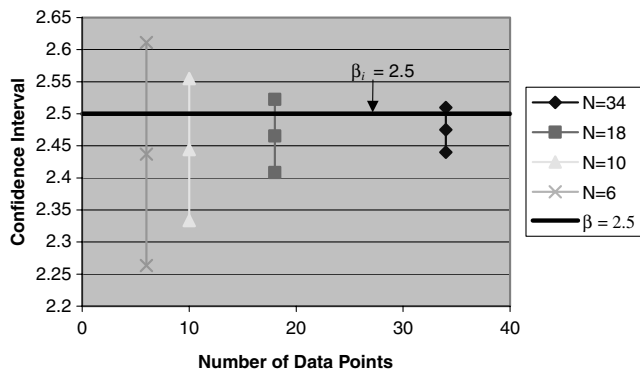


Fig. 2 Decreasing 95% confidence interval with increasing number of data points for the constant in $p_6(x, y)$ (Table 1).

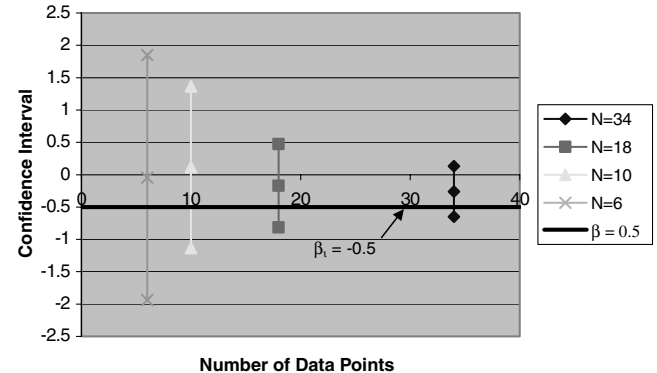


Fig. 3 Decreasing 95% confidence interval with increasing number of data points for the y coefficient in the function $p_6(x, y)$ (Table 1).

practical application, these specific functions could be obtained from a historical and/or theoretical database. Additionally, weights can be employed based on frequency of occurrence of these load distributions under known external constraints (e.g., weather, flight type).

Random functions were then chosen to provide a distributed load on the surface. The strains obtained were used in the current method to determine the possible Fourier coefficients [i.e., $\{a\}$ in Eq. (7)] for these functions. Minimization of Eq. (10) allowed for selection of the function in the database that was most similar to the unknown function. The similarity was not necessarily in equation form (e.g., exponential, quadratic), but in terms of the distribution over the intervals $[0, 2]$ in the x direction and/or $[0, 0.5]$ in the y direction. The appropriateness of the selected functions was verified with surface plots shown in Figs. 4 and 5. Figure 4 illustrates the function $1 - y$ recovered from a single Fourier approximation database (functions in Table 1), along with linear and quadratic functions from the database. Though the database contained a linear function in y , the method selected the quadratic function in y .

Figure 5 shows relative surface plots of the functions $2 + 3xy$ and the function $2 + 3xy^2$; the latter was recovered from the double Fourier database (Table 2) using the function $2 + 3xy$ as a test function. Figure 6 shows a surface plot of these four other functions in the database as well as their Fourier approximations for three terms ($n = 3$). A visual comparison of all plots indicates that the load distribution $2 + 3xy^2$ most closely matches the test function $2 + 3xy$ over the x interval $[0, 2]$ and y interval $[0, 0.5]$.

Flight load distributions on airfoils are usually represented as a function along the wingspan and along the chord. Allison and Mineck [12] and Iglesias [13] show realistic examples of such load distributions. These load distributions can be represented using the double Fourier approximation with $n = 3$.

Also, because actual strain data will have some variability, the regression analysis including function recovery was further tested for strain data with an error of $\pm 10\%$. It was observed that the method selected the correct function in all cases with this error.

C. Recovery of Functions on Large Structures

The study of the influence of data points revealed that an increased variance of the data set or an increase in the number of data points allows more accurate recovery of the a_{ij} s. A larger structure introduces the following components to the methods efficacy:

- 1) Fewer data points decrease the amount of data available for processing which may decrease the confidence intervals when obtaining the a_{ij} s.
- 2) The availability of more potential sensor locations provides an opportunity to obtain greater variance in the data set; this would improve the accuracy of coefficient recovery.

Whether 1 or 2 has a stronger influence on the success of function recovery is dependent on the expected load functions, the location of the strain sensors, and the lifting body material and geometric properties. If a minimum number of strain sensors are strategically placed such that the variance of the data set is comparable to that obtained with a larger data set that has provided theoretical function recovery, the method will also capture the expected loads with the smaller data set. For this to be realistically implemented, a FEA study could be done using the minimum locations under consideration. In this work, the dimensions of the finite element model were increased to $5 \times 3 \times 0.15 \text{ m}^3$; 90% of the coefficients of the functions in Table 2 were recovered with 10 data points to within 20% of their actual value. Note that the coefficients do not necessarily have to be recovered very accurately for the method to recover a function from the database that closely matches the expected load function. In the previous section, though the error in obtaining a single coefficient was as much as 23%, the method still selected the most appropriate function.

D. Time-Dependent Loads

This paper looks at static loading conditions. However, cyclic loads are important for fatigue analysis. Dynamic finite element

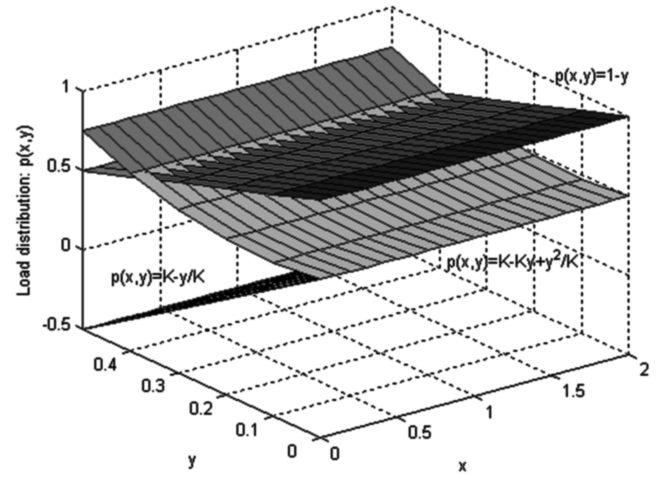


Fig. 4 Surface plot of the test function $1 - y$; the current method selected the quadratic function in y within the database. Though quadratic, this function is a better approximation than the only linear function in y in the database.

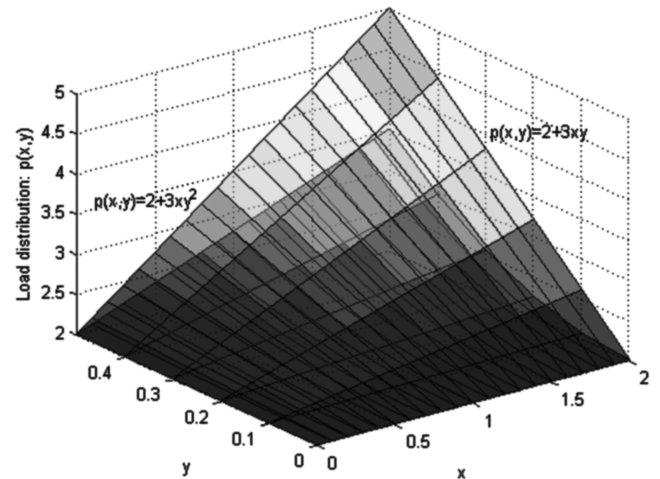


Fig. 5 Surface plot of the test function $2 + 3xy$; the current method selected the function $2 + 3xy^2$ in the database from Table 2.

analysis can be used to study the effect of such loads. For instance, one can express the i th load approximation as

$$F_i(s, t) = \sum_{j=1}^l a_{ij} R_{ij} \phi(t) \quad (13)$$

Using Eq. (13) in the finite element method, one can obtain the displacement and strain data at each time step. A least-squares regression analysis is performed at each time step in conjunction with the load function recovery algorithm. The proposed method is computationally intensive. However, given the cyclic characteristic of these loads, one might be able to identify the periodicity of the strain data, which in turn helps with the flight load identification process. The authors propose to study such loads in the future.

V. Conclusions

An inverse method based on finite element strain values successfully predicted Fourier and polynomial coefficients that enable comparison of unknown load distributions to a historical or theoretical database. The comparison, which implements the multiple least-squares method, has enabled successful selection of an unknown function from two types of databases. The first database consists of single Fourier coefficients, which approximate functions of one variable; the second consists of double Fourier coefficients, which approximate functions of two variables. It has been shown that

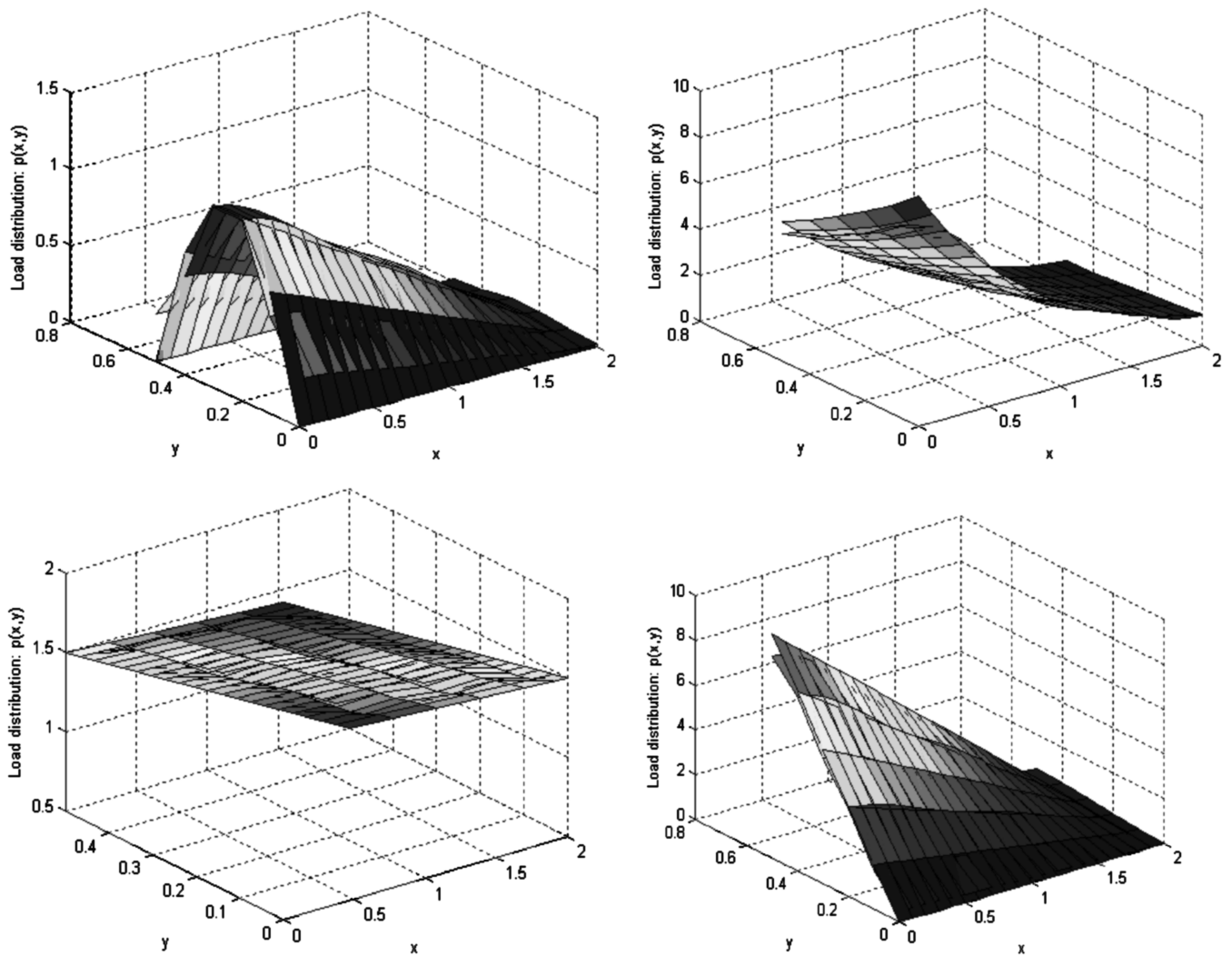


Fig. 6 Surface plot of the other functions in the database along with their Fourier approximations for $n = 3$.

the method is sensitive to the variance of the data set, the size of the data set, and the number of Fourier terms used to model the unknown function as well as the functions in the database. It is therefore important that the expected functions have the ability to be accurately modeled by the Fourier series with a small number of terms ($n = 2$) if the strain data set is relatively small ($N = 34$).

Acknowledgment

The authors wish to thank Cassandra Kim, an undergraduate engineering student, for her assistance with the generation of various finite element models in I-DEAS and her efficient use of Microsoft EXCEL for data organization and analysis.

References

- [1] Shkarayev, S., Krashantisa, R., and Tessler, A., "An Inverse Interpolation Method Utilizing In-Flight Strain Measurements for Determining Loads and Structural Response of Aerospace Vehicles," NASA TR 31WSHM, 2001.
- [2] Coates, C. W., Thamburaj, P., and Kim C., "An Inverse Method for Selection of Fourier Coefficients for Flight Load Identification," *Proceedings of the 46th Annual AIAA/ASME/ASCE/AHS Structures, Structural Dynamics and Mechanics Conference*, AIAA, Reston, VA, 18–21 April 2005.
- [3] Maniatty, A. M., Zabarbas, N., and Stelson K., "Finite Element Analysis of Some Inverse Elasticity Problems," *Journal of Engineering Mechanics*, Vol. 115 No. 6, 1989, pp. 1303–1317.
- [4] Maniatty, A. M., and Zabarbas, N. J., "Investigation of Regularization Parameters and Error Estimating in Inverse Elasticity Problems," *International Journal of Numerical Methods in Engineering*, Vol. 37 No. 6, 1994, pp. 1039–1052.
- [5] Tarantola, A., *Inverse Problem Theory: Methods for Data Fitting and Model Parameters Estimation*, Elsevier, New York, 1987.
- [6] Bogert, B. P., Haugse, E., and Gehrki, R. E., "Structural Shape Identification from Experimental Strains Using A Modal Transformation Technique," *44th AIAA/ASME/ASCE/AHS Structures, Structural Dynamics, and Materials Conference*, AIAA, Reston, VA, 7–10 April 2003.
- [7] Kirby, G. C., Lim, T. W., Weber, R., Bosse, A. B., Povich, C., and Fisher, S., "Strain Based Shape Estimation Algorithms for a Cantilever Beam," *Proceedings of SPIE Conference on Smart Structures and Materials*, SPIE—International Society for Optical Engineering, Bellingham, WA, March 1997.
- [8] Tessler, A., and Spangler, J., "An Inverse FEM for Application to Structural Health Monitoring," *Proceedings of the 14th U.S. National Congress of Theoretical and Applied Mechanics*, USNCTAM, Blacksburg, VA, 23–28 June 2002.
- [9] Cao, X., Sugiyama Y., and Mitsui, Y., "Application of Artificial Neural Networks to Load Identification," *Computers and Structures*, Vol. 69 No. 1, 1998, pp. 63–78. doi:10.1016/S0045-7949(98)00085-6
- [10] Myers, R. H., *Classical and Modern Regression Analysis*, 2nd ed., Duxbury Press-Wadsworth Publishing Co., Belmont, CA, 1990, Chap. 2.6.
- [11] Navidi, W., *Statistics for Engineers and Scientists*, 1st ed., McGraw-Hill, New York, Chap. 7.3.
- [12] Allison, D. O., and Mineck, R. E., "Aerodynamic Characteristics and Pressure Distributions for an Executive-Jet Baseline Airfoil Section," NASA TM 4529, 1993.
- [13] Iglesias S., "Optimum Spanloads Incorporating Wing Structural Considerations and Formation Flying" M.S. Thesis, Virginia Polytechnic Institute and State University, Blacksburg, VA, 2000.